1D Convolutional Neural Networks for Estimation of Compensatory Reserve from Blood Pressure Waveforms

Robert W. Techentin[1], Christopher L. Felton[1], Taylor E. Schlotman[4], Barry K. Gilbert[1], Michael J. Joyner[2], Timothy B. Curry[2], Victor A. Convertino[4], David R. Holmes, III[3], and Clifton R. Haider[1]

***Abstract*— We propose a Deep Convolutional Neural Network (CNN) architecture for computing a Compensatory Reserve Metric (CRM) for trauma victims suffering from hypovolemia (decreased circulating blood volume). The CRM is a single health indicator value that ranges from 100% for healthy individuals, down to 0% at hemodynamic decompensation – when the body can no longer compensate for blood loss. The CNN is trained on 20 second blood pressure waveform segments obtained from a finger-cuff monitor of 194 subjects. The model accurately predicts CRM when tested on data from 22 additional human subjects obtained from Lower Body Negative Pressure (LBNP) emulation of hemorrhage, attaining a mean squared error (MSE) of 0.0238 over the full range of values, including those from subjects with both low and high tolerance to central hypovolemia.**

I. INTRODUCTION

Hemorrhage is the leading cause of death from trauma [1]. Early intervention to prevent hemodynamic collapse is complicated by physiologic mechanisms that compensate for blood loss, maintaining, or nearly maintaining standard vital signs such as systolic blood pressure despite ongoing blood loss. New metrics of health status for trauma victims are required to enable timely and effective treatment, particularly when medical resources are limited and patients triage must be prioritized.

To study hemodynamic compensation, a human model of hemorrhage was developed using a technology called Lower Body Negative Pressure (LBNP), in which the lower half of a healthy test subject's body is placed into a pressure chamber and subjected to negative atmospheric pressure [2]. Blood is drawn to the lower extremities, reducing central blood volume and emulating hemorrhage. When negative pressure is released, the subject quickly recovers. LBNP studies of hypovolemia have led to the development of the concept of Compensatory Reserve [3] describing the body's ability to compensate for blood loss. Compensatory Reserve is reported as 100% reserve for healthy individuals, down to 0% reserve at the point of hemodynamic decompensation.

In this paper we present the development of a computational model for estimating a Compensatory Reserve Metric (CRM) from blood pressure waveforms based on Deep Convolutional Neural Networks (CNNs). Unlike techniques that require significant feature engineering, painstakingly extracting dozens [4] or hundreds or even thousands [5] of biological or statistical parameters from waveforms , deep CNNs automatically learn the relevant features from the waveforms themselves. While CNNs have been amazingly successful in recent years at image analysis [6], they are notorious for having a voracious appetite for training data. It is worth noting that this technique develops an effective CRM model from a dataset of only 222 human subjects.

[1]Special Purpose Processor Development Group [2]Department of Anesthesiology [3]Biomedical Analytics and Computational Engineering Laboratory, Mayo Clinic, Rochester MN, [4]US Army Institute of Surgical Research, San Antonio, TX

II. METHOD

A. LBNP Experimental Data

The LBNP dataset was provided by the U.S. Army Institute of Surgical Research (USAISR) under a protocol approved by the Institutional Review Boards (IRBs) of both the USAISR and the Mayo Clinic. The dataset included physiologic recordings of 16 different signals from 222 subjects undergoing the LBNP protocol. Data for all subjects included continuous measurements of heart rate (HR) obtained from a standard lead-II electrocardiogram (ECG), peripheral capillary oxygen saturation (SpO_2) obtained using a Near Infrared Spectroscopy (NIRS) system, capnogram (or end tidal CO_2), the applied negative pressure in mmHg, and beat-to-beat systolic (SBP) and diastolic (DBP) blood pressures, measured noninvasively using an infrared finger photoplethysmograph (PPG; Finometer® Bood Pressure Monitor, TNO-TPD Biomedical Instrumentation, Amsterdam, The Netherlands). The Finometer® blood pressure cuff was placed on the middle finger of the left hand, which was laid at heart level and calibrated with a standard manual brachial blood pressure cuff. Recordings ranged from 9 to 60 minutes in duration with data acquired at 500 samples per second.

The experimental protocol applied progressively stepwise LBNP while subjects were in a supine position. LBNP experiments began with five minutes of baseline recording, without application of LBNP (i.e., 0 mmHg), followed by five minute periods with chamber pressures set at -15, -30, -45, and -60 mmHg, with additional decreases of -10 mmHg every five minutes until the onset of hemodynamic decompensation. In accordance with the IRB, the maximum level of LBNP exposure wast 5 minutes at -100 mmHg. No subject completed five minutes at -100 mmHg (i.e., all subjects reached hemodynamic decompensation). For each subject, the end point of the experiment was defined at the point of decompensation, i.e., identified as systolic arterial pressure (SAP) < 80 mmHg (class III shock) concurrent with reporting of symptoms such as bradycardia, gray-out (loss of color vision), tunnel vision, sweating, nausea, or

978-1-5386-1311-5/19/$31.00 ©2019 IEEE

dizziness. Upon reaching this endpoint, the chamber vacuum was immediately released to ambient pressure, returning the subject to their baseline physiological status by rapidly restoring the central circulatiing blood volume.

The top panel of Figure 1 shows the applied LBNP and continuous systolic blood pressure recordings obtained from the Finometer® over the duration of the experiment for one subject. The inclusion of SBP highlights the need for the development of this algorithm. Shock is usually described clinically by severe hypotension, or SBP < 90 mmHg [7], though using this metric and similar standard vital signs can be misleading to the process of diagnosis. The figure shows that SBP remains within normal clinical values over the course of progressive central hypovolemia because it is tightly regulated by various compensatory mechanisms. It is therefore obvious that if the progression of hypovolemia is not arrested, the reserve to compensate is depleted and decompensation occurs. At decompensation, the SBP plummets, signaling the exhaustion of compensatory feedback mechanisms. It is clear from the recording in Figure 1 that tracking a signal that represents the underlying compensatory response provided by the CRM algorithm developed in this paper, a signal that changes immediately at the onset of blood loss, will avoid delays in recognition of the impending "crash" of SBP.

We selected 216 subjects with complete Finometer® waveform recordings for this model development. Although no demographic information was available, we know from the LBNP experimental results that the subjects were a mixture of high tolerance and low tolerance individuals [8], [2], where low tolerant individuals fail to complete the LBNP protocol through -60 mmHg and high tolerant indidividuals do complete this step. The machine learning algorithm developed in the following sections automatically accounts for high and low tolerance by predicting CRM as a percentage of the subject's individual tolerance.

B. Machine Learning Framework

We created a software framework for managing experimental data and running machine learning experiments. The 216 subjects were divided into training and test sets of 194 and 22, respectively. Defining training and test in terms of individual subjects is necessary, as we have observed over fitting (high variance) in cases where validation waveforms were selected from the pool of all subjects. Machine learning regression algorithms were trained to estimate CRM, in the range of 100% at baseline down to 0% at decompensation, from blood pressure waveform samples.

Supervised training of a regression algorithm to estimate CRM requires a training target, which must be calculated from the experimental data. Compensatory reserve cannot be directly measured, but we can define CRM training targets from the experimental data, defining the subject's CRM as 100% during the first five minutes of baseline recordings (i.e., LBNP of 0 mmHg) and defining CRM as 0% at the point of decompensation. This percentage represents the abstract concept of an individual subject's remaining capacity

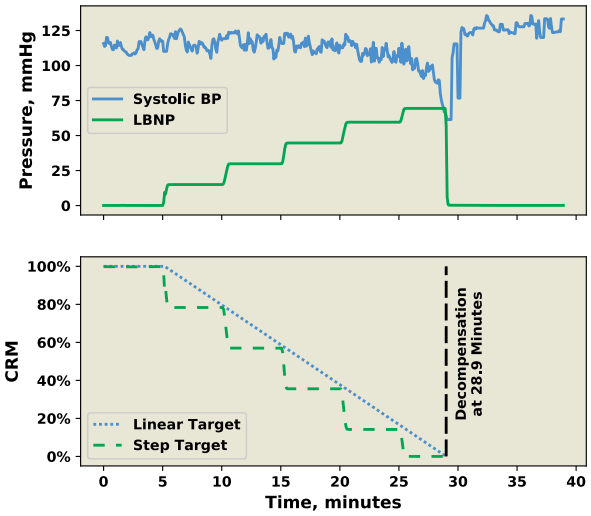

Fig. 1. Linear and Step Training Target Calculations for Subject A157

to compensate, or the capacity to protect against central hypovolemia, such that the reserve to compensate can be defined as the difference between the maximal response and the baseline state [9]. This exploits a key feature of this experimental dataset, in which all subjects were taken to the point of decompensation, discovering their individual tolerance to LBNP. With the endpoints defined, we can properly label each point in time with a target CRM for supervised machine learning. We can model decreasing CRM either as a linear function over the duration of the LBNP experiment, or as a series of steps corresponding to the applied LBNP. As an example, linear and stepped training targets for subject A157 are plotted in the bottom panel of Figure 1, along with the corresponding applied LBNP and SBP in the top panel. The point of decompensation at 28.9 minutes was derived from the release of LBNP. Note that the model is trained only on data before decompensation, as the target CRM is not known during recovery.

Once the endpoint and training targets were defined, the recorded Finometer® waveforms were truncated to the experiment length and divided into equal segments. Segments lengths of 20 seconds captured several heart beats and respiration cycles. Each waveform segment was associated with a step-wise CRM training target, as well as the subject identifier and a binary flag marking the point of decompensation. The last two were required for post-training analysis to compute area under the receiver operating characteristic curve using the Generalized Estimating Equation approach (GEE) [10].

The resulting training data included 30,075 training sample waveforms and 3,290 testing samples, based on the 194 and 22 subjects in the respective training and test sets. As each waveform sample is a one-dimensional time series data structure, 1-D Convolutional Neural Networks (CNNs) were trained using 90% of the training data, reserving 10%

for validation, which drove architecture selection. The loss function was mean squared error (MSE) comparing the predicted CRM to the training target for each waveform segment. Once a "good" architecture was found, it was re-trained on the entire training set and its fitness was evaluated with the reserved test data.

C. CNN Architecture Selection

Convolutional Neural Networks were trained and tested using Python and Keras, with the Tensorflow back end. The Keras library enabled relatively simple demonstrations of modestly complex CNN models that performed well for predicting CRM from LBNP blood pressure waveforms. A number of hand crafted models were evaluated, with varying numbers of convolutional layers, max pooling and dropout layers, with varying success.

However, the best architectures for 1-D CNN analysis of biologic waveforms are not obvious. In order to explore a number of possible architectures, we employed the hyperopt package [11] to find good values for the number of layers, numbers of filters, kernel sizes, and other parameters. Hyperopt is a Python library for optimizing over awkward search spaces with real-valued, discrete, and conditional dimensions. We chose Tree of Parzen Estimators (TPE) to explore a high dimensional parameter space, where discrete parameters could be random choice or random integer, and real-valued parameters could be derived from uniform or log, normal, or log-normal distributions. The layers and characteristics of the CNN were defined in terms of a hyperspace of these parameters, employing the layer stack shown in Figure 2.

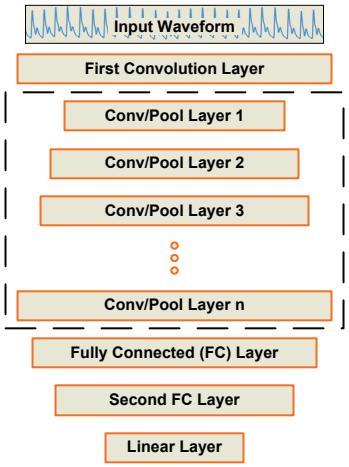

Fig. 2. Parameterized Layer Structure of Convolutional Neural Network

The first convolutional layer was defined separately from the other layers, as it must adapt to specific characteristics of the waveform data, and may have different kernel size and stride from the rest of the model. The bulk of the network is a block of convolutional/pooling layers, with the same kernel size and stride, and an increasing number of filters for each layer. Within this group, the convolution layer is followed by optional batch normalization [12], an optional residual layer [13], then parameterized pooling and dropout. The convolution layer group was followed by one or two fully connected layers and a final linear unit to compute CRM. Global model parameters included learning rate, L2 regularization factor, batch size, choice of optimizer, dropout probability, pooling type, and activation function.

Approximately one thousand candidate architectures were trained for 100 epochs and evaluated using mongodb for parallel execution on a Cray Urika GX supercomputer. It was clear from evaluating the results that several parameters should be fixed, and not subject to further optimization. For example, the swarm plot in Figure 3 has one point per trial, , grouped by pooling type, and shows that the optimizer developed a preference for max pooling over average pooling. This preference was validated by examining the training loss scores grouped by pooling type. It was also determined that batch normalization should always be included, the 'Nadam' optimizer should be used, and the activation function should always be the Rectified Linear Unit (relu).

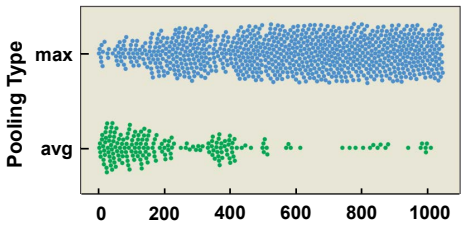

Fig. 3. Pooling type chosen by hyperopt over 1,000 trials, indicating a strong preference for "max" pooling

The hyper parameter search space was modified according to the results of the first thousand trials, and an additional two thousand candidate architectures were evaluated. From those evaluations, the 120 architectures with the best validation scores were analyzed to select the best overall hyperparameters. From that analysis, we derived a CNN architecture from parameters in Table I

TABLE I
HYPER PARAMETER VALUES FOR CRM CNN

Parameter	Value
First Conv Layer Filters	12
First Conv Layer Kernel Size	6
First Conv Layer Pool Size	4
Number of Conv/Pool Layers	7
Conv Filters Start	6
Conv Filters Multiplier	1.50
Conv Kernel Size	12
Conv Pool Size	3
Residual Layers	None
FC Layer 1 Units	565
FC Layer 2 Units	517
L2 Weight Regularization	0.00037
Learning Rate	0.000135
Batch Size	100

III. RESULTS

The resulting Convolutional Neural Network was reconstructed using Python and the Keras library. The model was re-trained on the entire training set of 194 subjects and 30,075 waveform samples for 200 epochs to produce a CRM model with MSE of 0.0236 and R^2 score of 0.8670. The CRM model was run on the test data of 22 subjects and 3,290 waveform samples to produce CRM scores for those LBNP experiments. The predictions were compared to the target CRM scores for the test subjects, yielding an overall MSE of 0.0238 and R^2 score of 0.8903. Predicted CRM and the stepped target CRM are plotted in Figure 4 for two test subjects; one high tolerance and one low tolerance. In this example, the low tolerance individual is distinctly different in his/her time to decompensation, compared to the high tolerage individual (25 vs 70 minutes, respectively). The CRM closely matches the stepped target, as would be expected from the low error score. Computed CRM for the high tolerance subject (A042) shows several spikes, both positive and negative, shortly after changes in LBNP. We found that these anomalies in the CRM were not caused by algorithm instability, but were in fact related to anomalies in the blood pressure waveform recordings, such as the one shown in Figure 5, during the baseline recording phase of the LBNP experiment. It is not clear from the waveform data if this anomaly is a true reflection of the subject's physiology, or if it was an artifact of the instrumentation and data collection, but it is clear that the algorithm can detect sudden changes in the blood pressure waveforms, whatever the cause.

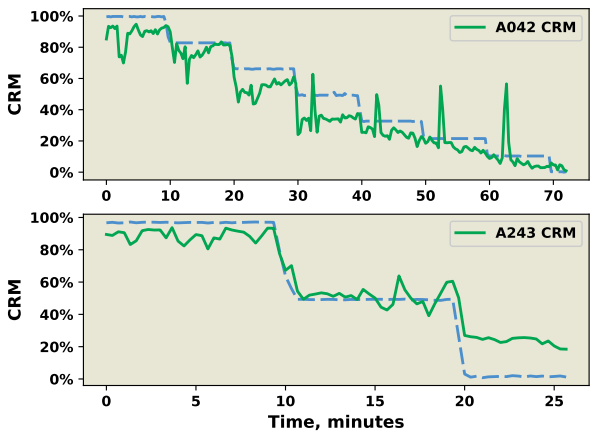

Fig. 4. Computed CRM compared to Stepped Training Target for One High Tolerance Subject (A042 - top panel) and One Low Tolerance Subject (A243 - bottom panel)

We applied the Generalized Estimating Equation method (GEE) to produce a Receiver Operating Characteristic (ROC) area under the curve (AUC) for the point of decompensation of 0.8910, as shown in Figure 6. This ROCAUC produced by the 1D CNN of the present study compares favorably with ROCAUCs generated from a previous machine-learning

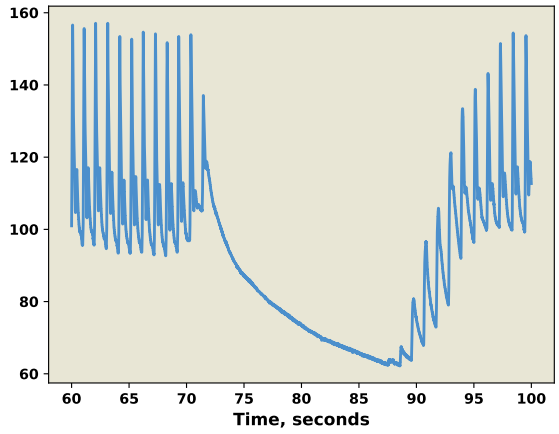

Fig. 5. Anomaly in Finometer® Blood Pressure Waveform for Subject A042 at 72 Seconds

algorithm of 0.90 for predictions of decompensation in an experimental human model of progressive central hypovolemia [14], [15], 0.79-0.83 for bleeding trauma patients [16], [17], [18], and 0.81-0.90 in humans with controlled blood loss [19], [20], [21]. This metric focuses only the CRM algorithm performance at the single point of decompensation, while the mean squared error (MSE) computed over the entire experiment is indicative of algorithm performance during a progressive hypovolemic episode.

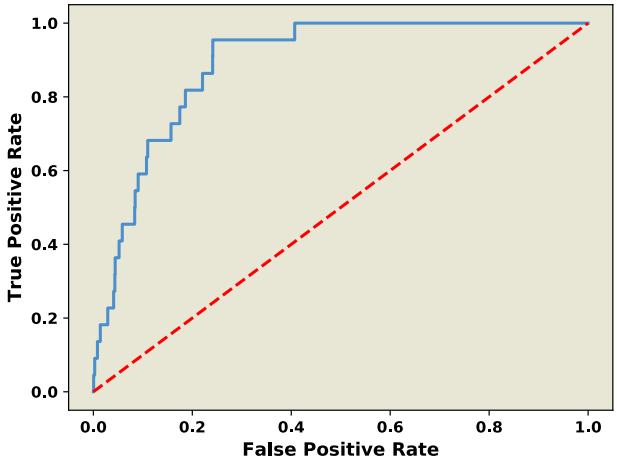

Fig. 6. Receiver Operating Characteristic (ROC) Curve for CRM Prediction of Decompensation Event. Area Under the Curve (AUC) = 0.8910

IV. CONCLUSIONS

A CNN model has been developed to compute Compensatory Reserve Metric in real time from blood pressure waveforms collected via Finometer® finger cuff. The CNN architecture was defined by parameters derived from thousands of candidate model trials. Performance of the model is robust compared to other techniques, and did not require extensive feature engineering. Further, this algorithm

is accurate for distinguishing subjects with low tolerance from subjects with high tolerance to central hypovolemia.

Future efforts will focus on demonstrating this model's accuracy, sensitivity and specificity on new data collected under different human experimental protocols as well as patients with a variety of conditions that will allow for "teaching" the algorithm to be diagnostic. We also will evaluate techniques for optimizing the algorithms to enable deployment in laboratory and clinical settings, as well as portable devices for field applications.

REFERENCES

[1] C. J. Carrico, J. B. Holcomb, and I. H. Chaudry, "Scientific priorities and strategic planning for resuscitation research and life saving therapy following traumatic injury: report of the pulse trauma work group," *Academic emergency medicine*, vol. 9, no. 6, pp. 621–626, 2002.

[2] A. M. Schiller, J. T. Howard, and V. A. Convertino, "The physiology of blood loss and shock: New insights from a human laboratory model of hemorrhage," *Experimental Biology and Medicine*, vol. 242, no. 8, pp. 874–883, 2017.

[3] S. L. Moulton, J. Mulligan, G. Z. Grudic, and V. A. Convertino, "Running on empty? the compensatory reserve index," *Journal of Trauma and Acute Care Surgery*, vol. 75, no. 6, pp. 1053–1059, 2013.

[4] S.-Y. Ji, W. Chen, K. Ward, C. Rickards, K. Ryan, V. Convertino, and K. Najarian, "Wavelet based analysis of physiological signals for prediction of severity of hemorrhagic shock," in *Complex Medical Engineering, 2009. CME. ICME International Conference on*. IEEE, 2009, pp. 1–6.

[5] F. Hatib, Z. Jian, S. Buddi, C. Lee, J. Settels, K. Sibert, J. Rinehart, and M. Cannesson, "Machine-learning algorithm to predict hypotension based on high-fidelity arterial pressure waveform analysis," *Anesthesiology: The Journal of the American Society of Anesthesiologists*, 2018.

[6] G. Litjens, T. Kooi, B. E. Bejnordi, A. A. A. Setio, F. Ciompi, M. Ghafoorian, J. A. Van Der Laak, B. Van Ginneken, and C. I. Sánchez, "A survey on deep learning in medical image analysis," *Medical image analysis*, vol. 42, pp. 60–88, 2017.

[7] A. C. of Surgeons, *Advanced Trauma Life Support (ATLS) Student Manual*. American College of Surgeons, 2012.

[8] V. A. Convertino, G. Grudic, J. Mulligan, and S. Moulton, "Estimation of individual-specific progression to impending cardiovascular instability using arterial waveforms," *Journal of Applied Physiology*, vol. 115, no. 8, pp. 1196–1202, 2013.

[9] V. A. Convertino and M. N. Sawka, "Wearable technology for compensatory reserve to sense hypovolemia," *Journal of Applied Physiology*, vol. 124, no. 2, pp. 442–451, 2017.

[10] G. A. Ballinger, "Using generalized estimating equations for longitudinal data analysis," *Organizational research methods*, vol. 7, no. 2, pp. 127–150, 2004.

[11] J. Bergstra, D. Yamins, and D. D. Cox, "Making a science of model search: Hyperparameter optimization in hundreds of dimensions for vision architectures," 2013.

[12] S. Ioffe and C. Szegedy, "Batch normalization: Accelerating deep network training by reducing internal covariate shift," *arXiv preprint arXiv:1502.03167*, 2015.

[13] C. Szegedy, S. Ioffe, V. Vanhoucke, and A. A. Alemi, "Inception-v4, inception-resnet and the impact of residual connections on learning." in *AAAI*, vol. 4, 2017, p. 12.

[14] J. T. Howard, J. C. Janak, C. Hinojosa-Laborde, and V. A. Convertino, "Specificity of compensatory reserve and tissue oxygenation as early predictors of tolerance to progressive reductions in central blood volume," *Shock*, vol. 46, no. 3S, pp. 68–73, 2016.

[15] J. C. Janak, J. T. Howard, K. A. Goei, R. Weber, G. W. Muniz, C. Hinojosa-Laborde, and V. A. Convertino, "Predictors of the onset of hemodynamic decompensation during progressive central hypovolemia: comparison of the peripheral perfusion index, pulse pressure variability, and compensatory reserve index," *Shock*, vol. 44, no. 6, pp. 548–553, 2015.

[16] M. C. Johnson, A. Alarhayem, V. Convertino, R. Carter III, K. Chung, R. Stewart, J. Myers, D. Dent, L. Liao, R. Cestero, *et al.*, "Compensatory reserve index: performance of a novel monitoring technology to identify the bleeding trauma patient," *Shock*, vol. 49, no. 3, pp. 295–300, 2018.

[17] ——, "Comparison of compensatory reserve and arterial lactate as markers of shock and resuscitation," *Journal of Trauma and Acute Care Surgery*, vol. 83, no. 4, pp. 603–608, 2017.

[18] A. Benov, O. Yaslowitz, T. Hakim, R. Amir-Keret, R. Nadler, A. Brand, E. Glassberg, A. Yitzhak, V. A. Convertino, and H. Paran, "The effect of blood transfusion on compensatory reserve: A prospective clinical trial," *Journal of Trauma and Acute Care Surgery*, vol. 83, no. 1, pp. S71–S76, 2017.

[19] V. A. Convertino, J. T. Howard, C. Hinojosa-Laborde, S. Cardin, P. Batchelder, J. Mulligan, G. Z. Grudic, S. L. Moulton, and D. B. MacLeod, "Individual-specific, beat-to-beat trending of significant human blood loss: the compensatory reserve," *Shock*, vol. 44, pp. 27–32, 2015.

[20] C. L. Stewart, J. Mulligan, G. Z. Grudic, V. A. Convertino, and S. L. Moulton, "Detection of low-volume blood loss: compensatory reserve versus traditional vital signs," *Journal of Trauma and Acute Care Surgery*, vol. 77, no. 6, pp. 892–898, 2014.

[21] R. Nadler, V. A. Convertino, S. Gendler, G. Lending, A. M. Lipsky, S. Cardin, A. Lowenthal, and E. Glassberg, "The value of noninvasive measurement of the compensatory reserve index in monitoring and triage of patients experiencing minimal blood loss," *Shock*, vol. 42, no. 2, pp. 93–98, 2014.